Natural Ventilation in Urban Areas -- Results of the European Project URBVENT
Part 1: Urban Environment

C. Ghiaus [*1], F. Allard[1], M. Santamouris[2], C. Georgakis[2], C.-A. Roulet[3], M. Germano[3], F. Tillenkamp[4], N. Heijmans[5], F. Nicol[6], E. Maldonado[7], M. Almeida[7], G. Guaracino[8], L. Roche[9]

[1]Université de La Rochelle, France
[2]National and Kapodistrian University of Athens, Greece
[3]Ecole Fédérale Polytechnique de Lausanne, Switzerland
[4]Axima Lab, Switzerland
[5]Belgian Building Research Institute, Belgium
[6]London Metropolitan University, UK
[7]Instituto de Engenharia Mecânica, Portugal
[8]ENTPE/CNRS Vaulx-en-Velin, France
[9]Building Research Establishment, UK

Abstract
The application of natural ventilation is more difficult in urban than in rural environment, especially in street canyons due to reduced wind velocity, urban heat island, noise and pollution, which are considered to be important barriers to the application of natural ventilation. The wind, temperature, noise attenuation and outdoor-indoor pollution transfer were measured in a large range of variation and various types of urban configuration. The models obtained can be used in the initial stages of building design in order to assess the viability of natural ventilation in urban environment, especially in street canyons.

Key words: street canyons, air flow, temperature, noise, pollution

1 Introduction

Urban environment has drawbacks for the application of natural ventilation: lower wind speed, higher temperatures due to the effect of urban heat island, noise and pollution. URBVENT project quantified some of these barriers.

The airflow in street canyons has much lower values as compared with the undisturbed wind. When the undisturbed wind has values larger than 2 to 4m/s, a correlation exists between it and the wind in the street canyons. When a 2m/s or stronger wind blows perpendicular to a street canyon, a vortex develops in the canyon. If the wind is parallel to the canyon axis, the vertical velocity in the canyon is very low. Based on existing information, completed with experimental data, an empirical model was developed for all types of undisturbed wind with velocity lower and higher than 4m/s.

The temperature measured inside the canyon streets was with about 5°C lower than that of the canopy layer, partially compensating the effect of the urban heat island.

Noise, another barrier for the application of natural ventilation, was studied in the same urban environment as the wind and the temperature. Based on experimental data, a simple model was developed to estimate the noise attenuation as a function of the height above the street level and the aspect ratio of the street canyon. A monogram, which is useful for decisions in the initial stages of the design, was obtained by making the assumption that the traffic

[*] Corresponding author. LEPTAB, University of La Rochelle, Av. M. Crépeau, 17000 La Rochelle cedex, France
Tel. +33 5 46457259; fax: +33 5 46458242
E-mail address: cristian.ghiaus@univ-lr.fr

intensity (and consequently the noise level) is dependent on street width. It was shown that the balconies reduce the noise level with about 2dB at the 1st floor and more than 3dB at the 4th floor.

Pollution is also considered to restrict the application of natural ventilation. Two aspects are important when pollution is analysed: first, the type and level of outdoor pollution is different as compared with the indoor; second, although initially the economical development increases the pollution level, when the financial and technological resources become available, the economical growth induces a reduction of the outdoor pollution [1, 2]. Experiments in URBVENT project and in the French related programme PRIMEQUAL showed that the indoor-outdoor pollutant ratio (I/O) depends on the facade airtightness and the outdoor concentration. Experiments were conducted for ozone, nitrogen dioxide and particle matter. The most important reduction was noticed for ozone, with I/O ratio of 0.05 to 0.33 (higher I/O ratio was measured for higher outdoor ozone concentration). The I/O ratio for nitrogen dioxide was between 0.05 and 0.95 with lower values for higher outdoor concentration. For particle matter, the I/O ratio was between 0.20 and 0.70, with values depending on the outdoor concentration and on the size of the particles.

2 Wind

The wind flow in street canyons had been studied especially for wind perpendicular to the canyon axis and for undisturbed wind having velocity higher than 4 m/s, e.g. [3-7], but also for parallel to canyon direction [8-12]. The more common case is when the wind blows at a certain angle relative to the long axis of the canyon. Unfortunately, the existing information on this topic is considerably smaller compared to perpendicular and along the canyon flows [9, 11-13]. To complete the information available, airflow measurements were carried out in URBVENT project for perpendicular, parallel and oblique direction to the canyon axis for five different urban canyons in the centre of Athens. The result is a concise model.

2.1 Modelling

When the wind speed outside the canyon is between 0.5 m/s and 4 m/s, although the flow inside the street canyon seemed to have chaotic characteristics, extended analysis of the experimental data resulted in two empirical models, one for wind blowing along the canyon and another for the wind blowing perpendicular or oblique to the canyon (Table 1).

If the wind speed outside the canyon is higher than 4 m/s, the wind inside the canyon depends on the incidence angle. When wind is parallel to the main axis of the canyon (incidence angle smaller than $\pm 15°$), the model of Nicholson [14] can be used. The inputs of this model are:

- air velocity (caps wind speed) outside the canyon and the wind incidence angle, g_w,
- canyon angle from north with values from 0-180°, g_c,
- mean building height, h_b, and the anemometer caps height, z_r,
- canyon width from wall to wall,
- a parameter related to the density of the buildings,
- height from the ground at which wind speed inside canyon is going to be estimated.

The outputs of the model are:

- value of the air velocity inside the canyon parallel to the canyon axis, up, at any height (from the ground to the mean building height),
- value of the air velocity inside the canyon perpendicular to the canyon axis, uc, at any height (from the ground to the mean building height),
- total air velocity inside the canyon, vi, where $vi = (up^2 + uc^2)^{0.5}$.

The equations used for calculation of upwind component are:

$$\bar{u} = \frac{u^*}{k} \cdot \ln \frac{z + p_d + z_0}{z_0}, \qquad (1)$$

and

$$u_p = U_0 \cdot \exp\left(\frac{y}{z_2}\right), \qquad (2)$$

where:

$\bar{u}$ is the mean wind in the free surface layer above roof tops,

u^* -frictional velocity,

k -Karman's constant (0.38),

p_d -zero-plane displacement,

z_0 -aerodynamic roughness length,

U_0 -constant reference speed,

z_2 -roughness length for the obstructed sub-layer,

y -height from ground at which we want to calculate the air velocity parallel to the canyon axis.

In order to calculate wind speed value inside the canyon, u_p, we should first calculate from equation (1) the value u^* (which is an unknown parameter) at height z, $z = z_r + h_b$, from ground level (where z_r is the cup anemometer height with a constant value of 10 meters and h_b is the mean building height) using as $\bar{u}$ the cup anemometer wind speed. After that, estimate, from the same equation (1) the $\bar{u}$ value for the h_b height (since now the u^* value is defined). From equation (2), calculate the U_0 value for the same height h_b, using also as input the previous calculated $\bar{u}$. This U_0 is now an input for equation (2), and, by defining the y value, which is the height from ground at which we want to calculate the wind, we can calculate the air velocity inside the canyon parallel to canyon axis, u_p. If we change the height y, because U_0 and z_2 are constant values, we can estimate from equation (2) the values of the air velocity at any height y (from ground level to the buildings height h_b).

When the wind incidence angle is perpendicular or oblique to the main axis of the canyon (± 15°), the air models of Hotchkiss and Harlow [15] and Yamartino and Wiegand [16] can be used. The inputs of these models are:

- air velocity (caps wind speed) outside the canyon and the wind incidence angle, g_w,
- canyon angle from north with values from 0-180° , g_c,
- mean building height, h_b, and the anemometer cap height, z_r,
- canyon width from wall to wall,
- coordinates (cross and along canyon) of the location inside canyon in which wind speed is going to be estimated (x , y).

The outputs of the model are:

- air velocity inside the canyon parallel to canyon main axis, u, at any height (from the ground to the mean building height),
- air velocity inside the canyon across to the canyon main axis, v, at any height (from the ground to the mean building height),
- air velocity inside the canyon vertical to canyon main axis, w, at any height (from the ground to the mean building height),
- air velocity inside the canyon at the horizontal level $w_h = (u^2 + v^2)^{0.5}$,
- total air velocity inside the canyon $w_t = (w_h{}^2 + w^2)^{0.5}$.

The equations used to calculate the wind components *v*, *w* are:

$$v = \frac{A}{k}\left[e^{ky}(1 + k \cdot y) - \beta \cdot e^{-ky} \cdot (1 - k \cdot y)\right] \cdot \sin(k \cdot x) \quad (3)$$

and

$$w = -A \cdot y \cdot \left(e^{ky} - \beta \cdot e^{-ky}\right)\cos(k \cdot x), \quad (4)$$

with

$$A = (k \cdot u_0)/(1 - \beta), \quad (5)$$

where k is Karman's constant (0.38), $\beta = e^{-2\,kD}$ where D is the depth of the canyon, which is the same with the mean buildings height, and u_0 is the wind speed value outside the canyon. The along canyon wind speed component is:

$$u = u_0 \cdot \log[(z + z_0)/z_0]/\log[(z_r + z_0)/z_0], \quad (6)$$

where u_0 is the wind speed value outside the canyon at reference height z_r and z_0 is the surface roughness.

When the wind speed value, u_o, is given, the values of β, k, A may be estimated. The cross velocity, *v*, results from equation (3) and the vertical velocity, *w*, from equation (4). The along canyon component of the velocity, *u*, results from equation (6).

The horizontal wind speed inside the canyon is:

$$v_h = (u^2 + v^2)^{0.5}. \quad (7)$$

The total wind speed inside canyon at the location of coordinates (x , y) is:

$$v_t = (v_h{}^2 + w^2)^{0.5}. \quad (8)$$

The models expressed by equations (1-(8) were integrated in an algorithm presented in Figure 1.

2.2 Model validation

The model presented in Figure 1 was validated by using the results of the experiments conducted in five street canyons in Athens under the conditions of hot weather and low wind velocity. After the validation of the model results, a very good agreement between the model and the experiments was found (Figure 2).

3 Temperatures

The temperature distribution in the urban canopy layer is greatly affected by the radiation balance. Solar radiation incident on urban surfaces is absorbed and then transformed into sensible heat. Most of the solar radiation impinges on roofs and on the vertical walls of buildings; only a relatively small part reaches ground level.

Analysis of the surface temperature has shown that the maximum simultaneous difference of the two facades was up to 10-20°C at the highest measured levels of the canyon, while the highest difference was close to 7°C at 20 meters above ground level. Comparison of the maximum difference of daily temperatures of the building facades and the surface temperature of the street shows that at street level temperature was 7.5°C higher than at the lower part of the canyon. The surface temperature stratification observed during the day period was between 30°C and 50°C on the South-East wall and between 27°C and 41°C on the North-West wall. The temperature differences between opposite surfaces during the day were higher at the highest location of the facade.

Regarding the air temperature stratification, at street level the temperature was 3°C higher than at the lower parts of the canyon but no specific temperature distribution pattern with the canyon height has been found. The absence of the stratification of the air temperature inside canyon agrees with the almost same mean values of the surface temperatures for all the measuring points in the canyon. A possible explanation for the temperature homogeneity in the space between buildings is the great advection. The fact that the air temperature outside the canyon is higher than inside is due to the street orientation which permits a lot of hours with shadow in the canyon and the very good airflow inside canyon due to the big aspect ratio (*H/W*=3.3).

4 Noise

High external noise levels often justify the use of air conditioning in commercial and residential buildings [17-20]. Methods of estimating noise levels in urban canyons are necessary if the potential for naturally ventilated buildings is to be assessed. These estimated noise levels can then be compared to the level of noise at which building occupants might be motivated to close windows in order to keep out the noise but also to compromise the natural ventilation strategy.

4.1 Noise measurements

A series of daytime noise measurements were made in 'canyon' streets in Athens with aspect ratio (height/width) varying from 1.1 to 5.3. The main purpose of the measurements was to examine the vertical variation in noise in the canyons in order to give advice on natural ventilation potential. A simple model of the noise level has been developed using a linear regression analysis of the measured data. The model can be used to predict the fall-off (attenuation) of the noise level with height above the street level.

Noise was measured outside the windows of buildings in nine street canyons in different areas of central Athens between the 13th and the 18th of September 2001. The aim of these measurements was to assess the effect of the height of the measurement point above canyon floor on the noise level [21]. The measurements were taken in canyons with aspect ratio ranging between 1 and 5 and with a variety of traffic loads. Table 2 indicates the geometrical characteristics of the streets. Table 3 indicates the date and time of start of measurement, the numbers of different types of vehicles passing during the 15 minute recording session (heavy, light and motorcycle), the street width in metres, the aspect ratio, the presence of balconies (0 = none, 1 = one side of the street, 2 = both sides), the gradient of the street (+ for uphill), the typical traffic speed in km/h and whether the traffic was travelling in one or both directions.

4.2 Modelling

The traffic noise, as measured at various locations in the canyons, is a combination of the direct sound and quasi-reverberation in the canyon. The term quasi-reverberation is used to denote a type of reverberation which is not diffuse but consists primarily of flutter echoes between the facades lining the street. Thus, the sound pressure, p, is:

$$p^2 \propto P(dc + rc), \tag{9}$$

where P is the sound power, dc is the direct component of the sound and rc is the reverberant component.

The direct component may be treated in two ways depending on whether the traffic is considered as a line source (where the traffic stream is considered as the source) or point source (where each vehicle is separately responsible for the noise). For a line source, the direct component, dc, is inversely proportional to the distance from the source; for the point source, the direct component, dc, is inversely proportional to the square of the distance. If the street width is w and the height of the measuring position above the ground is h, assuming the source is in the middle of the road, the distance between source and receiver is:

$$d = \left((w/2)^2 + h^2\right)^{1/2}. \tag{10}$$

For the reverberant sound, the noise is related approximately to the absorption area. Strictly, this applies to diffuse sound sources and is only approximate in this context. The main area for absorption is the open top of the canyon which is assumed to be a perfect absorber and whose area per metre of street equals w, the width of the street. A further sophistication may be to include absorption of the road surface and facades. With an absorption coefficient of 0.05, this would be leading to the absorption area

$$\begin{aligned} W &= w + 0.05w + 2\times 0.05h \\ &= 1.05w + 0.1h \end{aligned}, \tag{11}$$

where w corresponds to the top of the canyon, $0.05w$ to the floor of the canyon, and $2\text{x}0.05h$ to the walls. Alternatively, if we use the aspect ratio (AR) of the street, the expression (11) becomes:

$$W = w(1.05 + 0.1\cdot AR). \tag{12}$$

The sound power is assumed proportional to the number of vehicles per hour, n. For line source, its expression is:

$$p^2 = a\frac{n}{d} + b\frac{n}{W} + c. \tag{13}$$

For point source, its expression is:

$$p^2 = a\frac{n}{d^2} + b\frac{n}{W} + c, \tag{14}$$

where a, b, and c are constants related to the direct component, the reverberant component and to any background environmental noise entering the canyon, respectively. In general, the contribution of c will be small. Measurements on the rooftop of a building in a pedestrian area behind vehicular streets in the centre of Athens gave L_{Aeq} = 55dB. In the vehicular streets, few noise levels below L_{Aeq} = 70dB were recorded and L_{90} averaged 66dB. The expressions were developed into the form:

$$L_p = 10\log_{10}\left(n\left(\frac{a}{d_1} + \frac{b}{W}\right) + c\right), \tag{15}$$

where, by the normal definition of sound level in dB, L_p, the noise level for a sound pressure level p, is equal to $10\log_{10} p$ and d_1 is d or d^2 (see equations (13) and (14)) depending on the assumption about the shape of the noise source.

In order to determine how these results accord with the theoretical model presented above, values were calculated for n/d (referred to as D), n/W (rv) and n/W (RV) in order that a linear regression can be conducted for p^2 from equations (13) and (14) with W as defined in equation (12). Regression analysis were performed for p^2 against combinations of these variables, initially to determine which combination has the best explanatory power.

The regression equation (13), for p^2 on D_2 (the value of D when the traffic is assumed to be a line source in the middle of the street) and RV using the data from the whole 15 minutes gives:

$$\begin{aligned} p^2 &= 17.4\times 10^4.D_2 \\ &+ 5.34\times 10^4.RV - 411\times 10^4 \end{aligned}. \tag{16}$$

Then,

$$L_{eq} = 10\log_{10} p^2, \tag{17}$$

where L_{eq} is the noise level at height h above the street; D_2 is a function of three variables, h, w and n, the number of vehicles (n assumed to be proportional to the noise generated). Two of these variables (n and w) are also included in RV together with the aspect ratio, AR, of the canyon. There is a logical problem with a negative value for c since the value of p^2 cannot be negative. This value may be due to a curvature in the relationship which the linear regression cannot take into account.

In order to facilitate the visualisation, a simplifying assumption has been made that the traffic level is a

function of street width. In these data, the correlation between traffic intensity, expressed in number of vehicles per hour, n, and street width w (m) was R=0.88 and the regression relationship was:

$$n = 137w - 306 . \quad (18)$$

Using this simplifying assumption, values of expected noise level at different heights for a particular value of street width, w, can be calculated (Figure 3). Assuming that the traffic in the canyons follows the relationship shown in equation (18), the expected daytime noise level becomes purely a function of the geometry of the street. Figure 3 shows the expected noise levels in Athens at different street widths and heights above the street streets and the implication of this for natural ventilation potential of office units at a height h above street level.

4.3 Conclusions

This is an initial study of the daytime traffic noise measurements in urban canyons in Athens. Further work is necessary, but from this study it is possible to draw a number of tentative conclusions.

1. High levels of noise can be found in these canyon-type streets and show a predominance in the low-frequency end of the noise spectrum despite a high proportion of motorcycles in the traffic mix.
2. The noise level in canyon streets increases with traffic density and decreases with height above the canyon floor.
3. The attenuation in noise level compared to that at street level increases with the distance from the canyon floor, but decreases with increasing street width.
4. These relationships are well represented by a simple model of noise level comprising a direct component and a reverberant component.
5. The direct component is assumed to be from a line source at or near the centre of the road whose power falls off with the inverse of the distance from this source.
6. The reverberant component is assumed to act as if the street were a two-dimensional room with the canyon roof acting as a perfect absorber. There may be a small additional noise component from the general environmental noise.
7. The simple model, calibrated from the measured data, shows that the noise attenuation (L_{Aeq}) is almost entirely a function of street width and height above the canyon floor.
8. The maximum value of the attenuation (and hence the best possible noise attenuation) is almost entirely a function of aspect ratio with a small effect of street width in narrow streets.
9. Similar considerations apply when predicting the attenuation of L_{10} and L_{90}. Relative to L_{eq}, the rate of attenuation with height is greater for L_{10} and less for L_{90}.
10. Figure 3 indicates the potential for natural ventilation of offices as a function of street width and height above the street
11. Simulations have been used to predict the reduction in noise level at the building surface afforded by balconies. The simulation suggests that the noise reduction due to balconies is about 2dB lower in buildings rising to 3-4dB near the top of the canyon.

5 Pollution

Outdoor air pollution is commonly considered as another barrier to natural ventilation since filters cannot be used as in mechanical or air-conditioning systems.

The indoor air quality is related to the outdoor air pollutant concentration through the rate of air change and reactivity of the pollutant [22-24]. The facade airtightness, as an intrinsic characteristic of the building, represents a key factor in this relation because it is the main link between the indoor and outdoor environments, being in the same time an important characteristic of the natural ventilation property of the building.

The key outdoor pollutants (SO_2, NO_2, CO, O_3, suspended particle matter, and lead) are usually monitored in large cities [25]. The mean levels of sulphur dioxide and lead are equal at indoors and outdoors. Ozone and nitrogen dioxide react with the building material resulting in a lower concentration indoors than outdoors, when the building is airtight. The particle matter transfer depends on the particle size. The experimental results show that the ratio between indoor and outdoor concentration (I/O) depends also on the outdoor concentration of the pollutant.

The indoor-outdoor ratio was studied for ozone, nitrogen dioxide and particle matter in the framework of the URBVENT project and of the related French programme PRIMEQUAL.

5.1 Experimental measurements

Two types of measurements were performed: one-time measurement of the facade permeability and continuos measurement of the indoor and outdoor pollution levels. Nine schools were selected in order to cover a wide range of urban environment, facade characteristics and types of ventilation system. The choice of the tested classrooms inside the schools was guided by practical reasons concerning the security of the pupils [26]. The wall covering materials, furnishing and cleaning procedures were roughly the same for all schools so that these parameters should not be considered in the study. For each school, two week campaigns were conducted, one in summertime and the other one in wintertime.

Facade permeability was measured for every classroom. It was calculated based on two permeability laws obtained by the false door method [27, 28]: one for the normal room and another for the sealed room. In both situations, the classroom was pressurised and depressurised. The change from the pressurised to the depressurised configuration was done by inverting the ventilation system. The airflow that crosses the facade of the classroom is equal to the airflow introduced through the ventilation duct crossing the false door. The indoor/outdoor pressure difference was measured with a micro-manometer. Each series of measurement contains six or more simultaneous measurements of the airflow and the indoor/outdoor pressure difference between 3 and 60 Pa. The permeability law of the classroom was obtained by regression between the measured couples (*Dp, Q*) for normal operation (total permeability) and sealed room (when the facade was sealed by Scotch-taping all the joints). The permeability laws of the facade were calculated as the difference between total permeability and the sealed room permeability.

The airtightness of the building facade, one of the two input parameters of the model, classifies the buildings in three groups: very permeable, permeable, and airtight (Figure 4). The airflow through the facade was estimated based on the facade permeability law and the pressure difference on the facade measured continuously and simultaneously with the other parameters.

The following variables were measured continuously: the pressure difference across the facade, the outdoor and indoor concentration of ozone, nitrogen dioxide, carbon dioxide, indoor temperature and humidity, state of the window (open or closed). The concentration of the indoor and outdoor suspended particle matter (PM) was sampled every minute by two light diffraction analysers with 15 channels for 0.3, 0.4, 0.5, 0.65, 0.8, 1, 1.6, 2, 3, 4, 5, 7.5, 10, 15, and 20 µm. The indoor temperature and the relative humidity were measured with sensors placed at 1m under the ceiling of the classroom. The state of the classroom windows (open or closed) was precisely recorded by means of magnetic sensors.

5.2 Modelling

The ratio of indoor-outdoor concentration (*I/O*) is a non-linear function of two variables: outdoor concentration and facade airtightness. Because the phenomena are continuous (no phase change, for example), the model should be continuous in values and in its derivatives. The non-linearity may be dealt with by calculating local models [29, 30].

The indoor - outdoor concentration ratio (I/O) is mapped on outdoor concentration, C_o, and the three main levels of airtightness of the facade: "airtight" ($Q_{4Pa} \approx 0 m^3/h$), "permeable" ($Q_{4Pa} \approx 150 m^3/h$) and "very permeable" ($Q_{4Pa} \approx 300 m^3/h$). The I/O ratio was determined for closed windows (measurements during night). Since the room volume was about 150m^3, the maximum air change per hour was about 2 ach.

The I/O ozone ratio diminishes with the outdoor concentration for the airtight facades and increases for the other two types of facades (Figure 5). Two clusters were found: the first is situated in the zone of the airtight facade ($c_{Q4Pa} \approx 5 m^3/h$) and middle-ranged outdoor concentration ($c_{Co} \approx 28 ppb$); the second one is placed in the zone of the "most permeable" facades ($c_{Q4Pa} \approx 292 m^3/h$) for middle-ranged outdoor concentration ($c_{Co} \approx 36 ppb$). The two peaks of the model are placed in the zone of "airtight" facade with low outdoor O_3 concentration and the zone of the "most permeable" facade with high outdoor O_3 concentration (Figure 5 *a*). The second map (Figure 5 *b*) presents the precision of the model expressed by the dispersion of the points in the database. The map shows that the smallest dispersion of the I/O value *0.18* while the higher dispersion is *0.38* (Figure 5 *b*). The third map presents the credibility of the first two maps (Figure 5 *c*). It is higher in the zones where more measurement points were collected, i.e. in the proximity of the two clusters. The highest credibility zone ($CR>0.5$) corresponds to the middle-ranged outdoor O_3 concentrations, between the centres of the two clusters, while the lowest credibility zones ($CR<0.25$) are for the "most permeable" facade with

low outdoor concentrations and "airtight" facade with high outdoor concentrations.

The same three parameters were calculated for nitrogen dioxide. The I/O ratio diminishes with the outdoor concentration regardless the facade airtightness. The values of the I/O ratios corresponding to the airtight facades are slightly higher then those corresponding to “permeable“ or “very permeable” facades (Figure 6 *a*). The model precision is almost the same for the whole domain (Figure 6 *b*). The credibility is higher in the zones where more measurement are available, i.e. in the proximity of the clusters. Two clusters were found for lower outdoor concentration (Co_{NO2}<15ppb): one cluster corresponds to the “airtight“ buildings and the second one corresponds to the “very permeable”. The credibility parameter diminishes with the rise of the outdoor concentration, having values between 0 and 0.5 for outdoor concentrations higher than 20ppb (Figure 6 *c*).

The same three values were estimated for the penetration indoors of three different sizes intervals of the particle matter: 0.3-0.4µm, 0.8-1µm and 2-3µm. Similar conclusions can be drawn for all three particle sizes.

The I/O ratios diminish with the outdoor concentration regardless the building facade airtightness or the size of the particles. For the size interval 0.3-0.4µm (Figure 7 *a*), the model surface is relatively plane, so the I/O ratio diminishes linearly with the outdoor concentration. For the other two sizes, the model maps present a concavity in the model surfaces for the small values of the outdoor concentration and the “permeable” facades (Figure 7 *d* and *g*). Contrary to the first two size intervals, the model surface of the class 2-3µm presents I/O ratios of 0.65 corresponding to high outdoor concentration and “very permeable” facade. However, the prediction credibility index is very small for that zone.

The dispersion of the I/O ratio presents almost constant values for all outdoor pollution range and facade permeability. The value of the index characterising this dispersion is about 0.33 for the first size interval (Figure 7 *b*), while it is twice higher for the last two size intervals (Figure 7 *e* and *h*). The prediction credibility presents the same diminishing trend with the outdoor concentration (Figure 7 *c*, *f* and *i*).

5.3 Conclusions

The outdoor and indoor pollution have different sources and usually refer to different types of pollutants. After a threshold in wealth is attained, when the financial and technological means become available, the outdoor pollution diminishes with the economic development.

In the joint framework of URBVENT project and the French programme PRIMEQUAL, an experimental study of outdoor - indoor pollution transfer was conducted in nine schools. The pollutants studied were ozone, nitrogen dioxide and 15 sizes of particle matter. Three maps were calculated for every pollutant: the I/O ratio, the precision of this estimation and the degree of confidence in the I/O ratio and precision. The ratio of indoor - outdoor concentration was determined as a function of airflow through the facade and of the outdoor concentration. The indoor concentration was smaller inside than outside. Ozone presented the lowest I/O ratio (0.1-0.4). The I/O ratio for nitrogen dioxide was between approximately zero and 0.95. The I/O ratio for particle matter depended on the particle size. The most important variation (0.25 - 0.70) was measured for particles of small size (0.3-0.4µm); particles of larger size (0.8 - 3µm) represented lower, but comparable, variation of the I/O ratio (0.3-0.7).

6 Acknowledgements

The URBVENT project was partly supported by the European Commission in the 5th Framework Programme in the field of research, technological development and demonstration. The indoor-outdoor pollution transfer study was supported by the French Government in the research programme PRIMEQUAL.

7 References

[1] Lomborg B. *The Skeptical Environmentalist.* 2001: Cambridge University Press.

[2] Shafik N. *Economic development and environmental quality: an econometric analysis*. Oxford Economic Papers, 1994; 46: 757-773.

[3] Albrecht F., Grunow J. *Ein Beitrag zur Frage der vertikalen Luftzirkulation in der Grossstandt.* Metorol, 1935(52): 103-108.

[4] Chang P.C., Wang P.N., Lin A. *Turbulent diffusion in a city street.* in *Symposium on Air Pollution and Turbulent Diffusion*. 1971. Las Cruces, New Mexico.

[5] DePaul F.T., Sheih C.M. *Measurements of wind velocities in a street canyon.* Atmospheric Environment, 1986; 20: 445-459.
[6] Hoydysh W., Dabbert W.F. *Kinematics and dispersion characteristics of flows in asymmetric steet canyons.* Atmospheric Environment, 1988; 22(12): 2677-2689.
[7] Lee I.Y., Shannon J.D., Park H.M. *Evaluation of Parameterizations for Pollutant Transport and Dispersion in an Urban street canyon using a three - dimensional dynamic flow model.* in *87th Annual Meeting and Exhibition*. 1994. Cincinnati, Ohio.
[8] Arnfield A.J., Mills G. *An Analysis of the circulation characteristics and energy budget of a dry, asymmetric, east, west urban canyon. I. Circulation Characteristics.* Journal of Climatology, 1994; 14: 119-134.
[9] Nakamura Y., Oke T.R. *Wind, temperature and stability conditions in an E-W oriented urban canyon.* Atmospheric Environment., 1989; 22(12): 2691-2700.
[10] Nurez M., Oke T.R. *The energy balance of an urban canyon.* Journal of Applied Meteorology, 1977; 16: 11-19.
[11] Santamouris M., et al. *Thermal and airflow characteristics in a deep pedestrian canyon under hot weather conditions.* Atmospheric Environment, 1999; 33: 4503-4521.
[12] Wedding J.B., Lombardi D.J., Cermak J.E. *A wind tunnel study of gaseous pollutants in city street canyons.* J. Air Pollut. Control Ass., 1977; 27: 557-566.
[13] Dabberdt W.F., Ludwig F.L., Johnson W.B. *Validation and applications of an urban diffusion model for vehicular emissions.* Atmospheric Environment, 1973; 20: 445-459.
[14] Nicholson S.E. *A pollution model for street-level air.* Atmospheric Environment, 1975; 9(1): 19-31.
[15] Hotchkiss R.S., Harlow F.H., *Air pollution and transport in street canyons*. 1973, Office of Research and Monitoring: Washington, D.C, US.
[16] Yamartino R.J., Wiegand G. *Development and evaluation of simple models for the flow, turbulence and pollution concentration fields within an urban street canyon.* Atmospheric Environment, 1986; 20: 2137-2156.
[17] Wilson M. *A Review of Acoustic Problems in Passive Solar Design.* in *EuroNoise '92*. 1992.
[18] Wilson M., Nicol F., Singh R. *Measurements of background noise levels in naturally ventilated Buildings associated with thermal comfort studies: Initial results.* Proc IOA, 1993; 15(8): 283-295.
[19] Dubiel J., Wilson M., Nicol F. *Decibels and discomfort- an investigation of noise tolerance in offices*. in *Joint CIBSE/ASHRAE confference.* 1996. Harrogate.
[20] Nicol F., Wilson M., Dubiel J. *Decibels and Degrees-interaction between thermal and acoustic interaction in offices*. in *CIBSE National Conference.* 1997.
[21] Nicol F., Wilson M., Shelton J. *The effect of street dimensions and traffic density on the noise level at different heights in urban canyons*. in *EPIC 2002, 'Energy Efficient & Healthy Buildings in Sustainable Cit*. 2002. Lyon, France.
[22] Hayes S.R. *Use of an Indoor Air Quality Model (IAQM) to Estimate Indoor Ozone Levels.* Journal Air & Waste Management Association, 1991; 41(2): 161-170.
[23] Weschler C.J., Shields H.C., Naik D.V. *Indoor Ozone Exposures.* JAPCA, 1989; 39: 1562-1568.
[24] Shair F.H., Heitner K.L. *Theoretical model for relating indoor pollutant concentrations to those outside.* Environmental Science And Technology Journal, 1974; 8(5): 444-451.
[25] WHO, *Air quality guidelines.* 2000, World Health Organisation: Geneva.
[26] Iordache V., *Etude de l'impact de la pollution atmosphérique sur l'exposition des enfants en milieu scolaire - Recherche de moyens de prédiction et de protection*, in *LEPTAB.* 2003, Université de La Rochelle: La Rochelle.
[27] ASTM, *Standard Test Method for Determining Air Leakage Rate by Fan Pressurization.* 1999: West Conshohocken, PA 19428-2959, US.
[28] Ribéron J. *Guide méthodologique pour la mesure de la perméabilité à l'air des enveloppes de bâtiments*. Cahiers du CSTB n° 2493. 1991, Paris: Centre Scientifique et Technique du Bâtiment. 21.
[29] Jang J.S.R., Sun C.T., Mizutani E. *Neuro-Fuzzy and Soft Computing. A Computational Approach to Learning and Machine Intelligence*. 1997, Upper Saddle River, NJ, US: Prentice Hall.
[30] Wonnacott T.H., Wonnacott R.J. *Introductory Statistics for Buissness and Economics*. 1990: John Wiley & Sons.

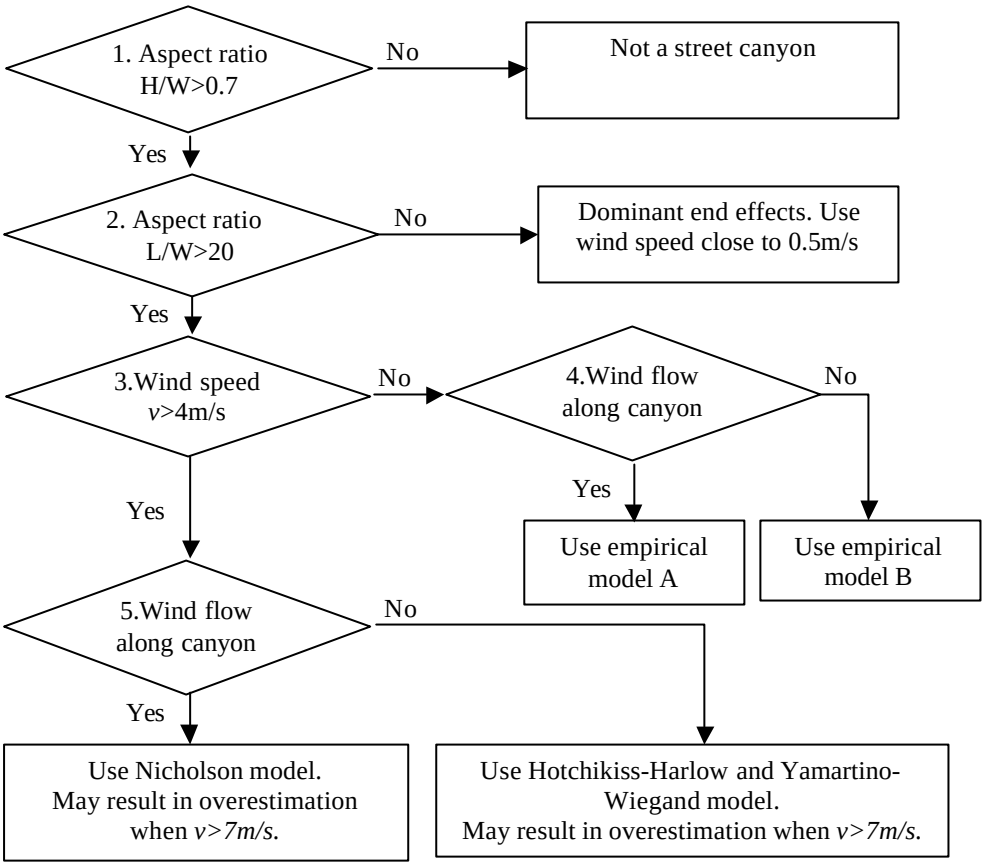

Figure 1 Algorithm for wind velocity in canyon streets

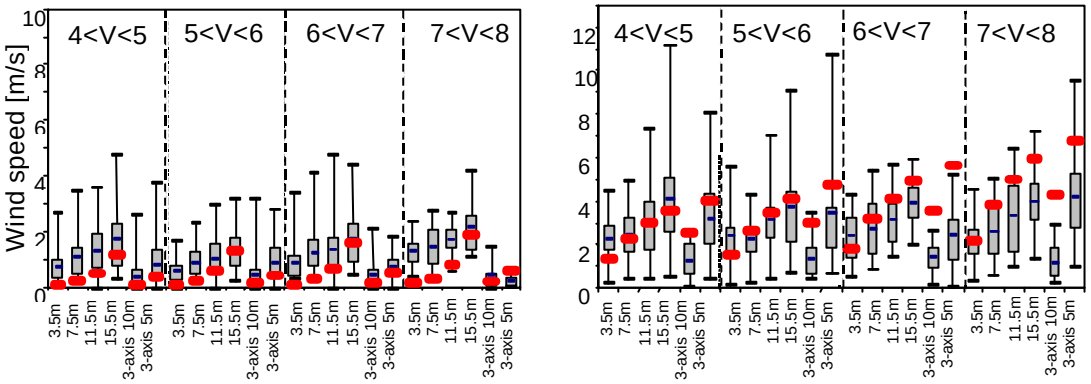

Figure 2 Examples of validation of wind speed in street canyons: a) Nicholson model; b) Hotchkiss model. The experimental data are shown by box-plots. The prediction of the model are figured in bold segments.

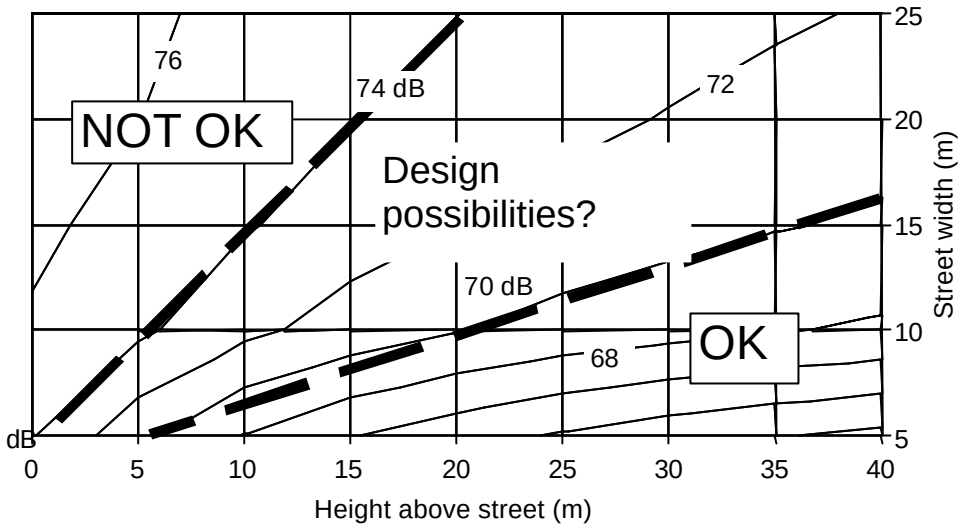

Figure 3. Contours of noise level at different heights above the street and street widths. Configurations in which natural ventilation is possible are indicated (OK), as are those in which it is ruled out (NOT OK). Between these two extremes is a region in which there are possibilities for design solutions

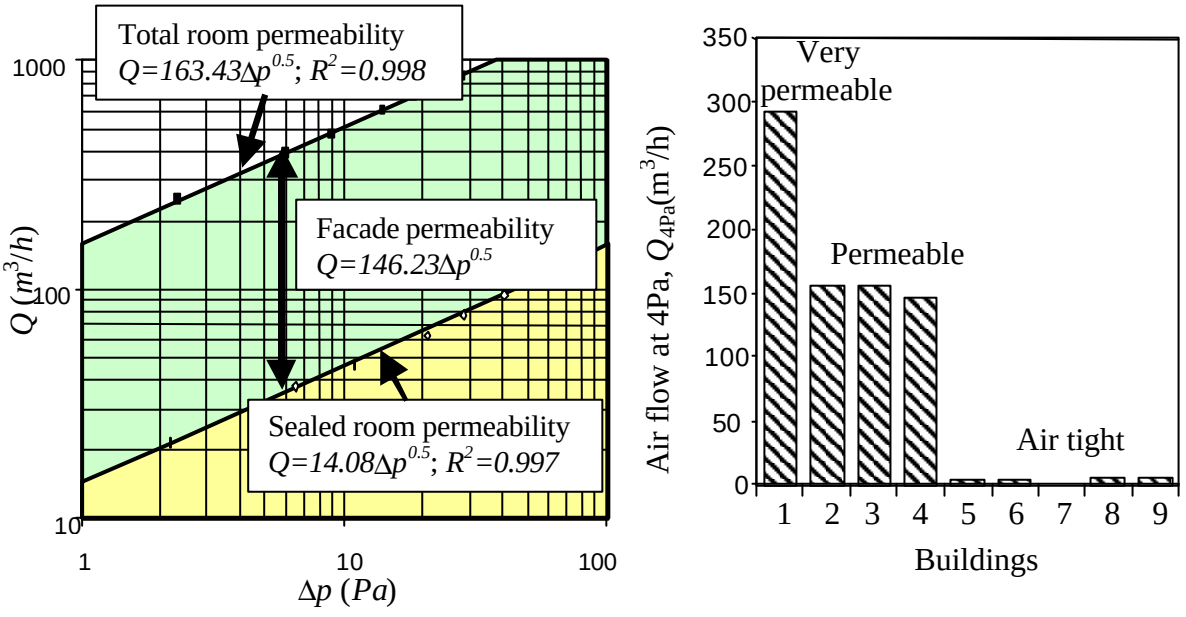

Figure 4. Building classification according to their permeability (Iordache 2003).

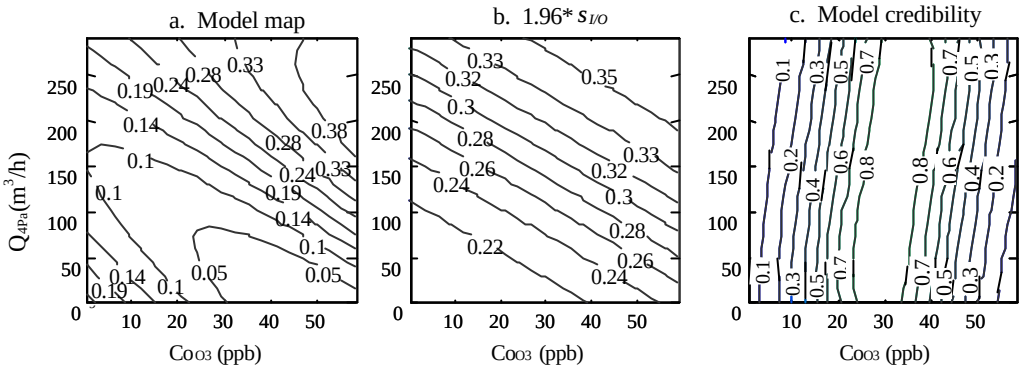

Figure 5 Ozone outdoor-indoor transfer: a) I/O ratio; b) precision; c) degree of confidence (Iordache 2003).

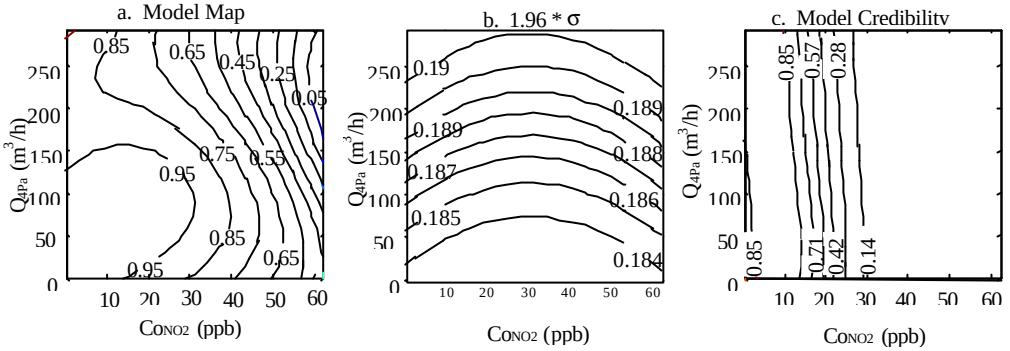

Figure 6 NO2 outdoor-indoor transfer: a) I/O ratio; b) precision; c) degree of confidence (Iordache 2003).

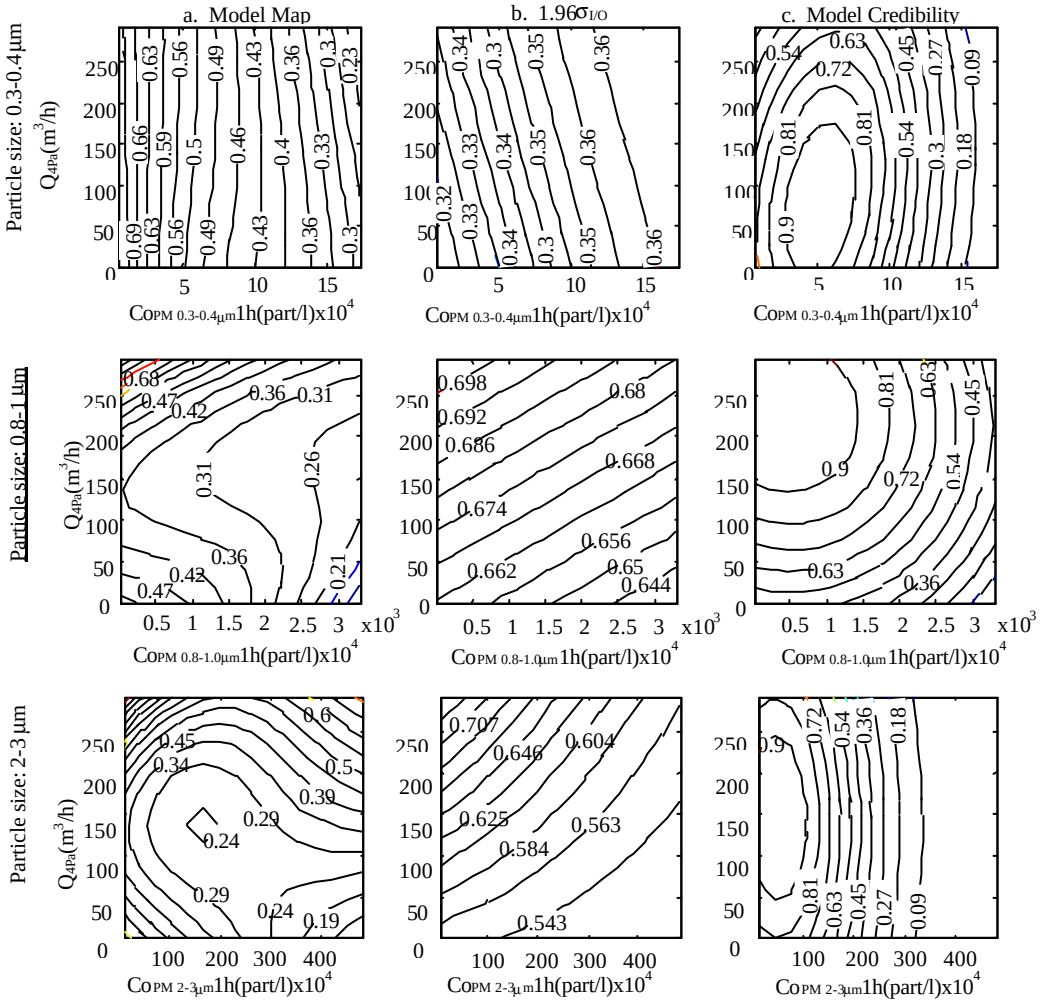

Figure 7 Particle matter outdoor-indoor transfer: a) I/O ratio; b) precision; c) degree of confidence (Iordache 2003).

Table 1 Values for air speed inside the canyon when the undisturbed wind speed is lower than 4 m/s

Wind speed outside the canyon (U)	Air speed inside the canyon				
	Wind bows along canyon		Wind blows perpendicular or oblique to the canyon		
	Typical values in canyon		Typical values in canyon		
			near the windward facade		near the upwind facade
	lowest part	highest part	lowest part	highest part	
$0<U<1$	0.3 m/s	0.7 m/s	0.4 m/s	0.7 m/s	0.4 m/s
$1<U<2$	0.4 m/s	1.3 m/s	0.4 m/s	1.3 m/s	0.4 m/s
$2<U<3$	0.4 m/s	1.5 m/s	0.6 m/s	1.5 m/s	0.6 m/s
$3<U<4$	0.4 m/s	2.2 m/s	0.7 m/s	3 m/s	0.7 m/s

Table 2 Height (in metres) of recording point above street level, and 15-minute L_{A90}, L_{Aeq} and L_{A10} for street level and each recording point for each street in the survey. Note that in street OCT only one measuring point is shown because of a failure in one noise level meter

	Metres above St		**L_{A90} dB**			**L_{Aeq} dB**			**L_{A10} dB**		
	Low	**High**	**Street**	**Low**	**High**	**Street**	**Low**	**High**	**Street**	**Low**	**High**
AKE	11.5	25.5	72.1	71.5	69.8	78.6	76.8	74.3	81.7	79.5	76.6
AME	11.5	22	70.1	69.1	64.9	77.8	74.8	69.9	80.7	77.4	72.2
HAR	8	11.5	62.8	63.2	63.1	74.9	71.6	70.3	77.8	74.3	73.2
MI1	8	12	63.8	63.5	62.1	73.2	69	67.3	75.3	71.1	69.4
MIM	18.5	22.5	64	63.2	61.5	72.9	69.7	65.6	75.1	71.9	67.6
OCT	33		70.6	68.7		81	77		81	76.9	
OTE	8	18.5	66.1	67.2	67.7	74.4	75.1	73.4	75.1	75.1	73.9
PED	15	22	62	59.8	55.4	66.1	63.2	57.8	68.5	65.5	59.9
SOL	11.5	15	66.9	66.3	64.8	76	73.2	71.9	79.1	76.1	74.7

Table 3 Basic data for the streets measured

Street	**Date**	**Time**	**Vehicles passing in 15min**				**Width**	**AR**	**Balc**	**Grade**	**Est speed**	**Traffic**
			Heavy	**Light**	**M/C**	**Total**	**Metres**				**km/hr**	**1/2-way**
AKE	17/09/01	11:55	32	386	356	774	19	1.6	0	0	0-40	2
AME	17/09/01	11:17	4	185	199	388	10	2.3	0	+5%	0-40	1
HAR	18/09/01	11:11	8	117	62	187	10	1.6	2	0	0-15	1
MI1	13/09/01	12:19	3	83	107	193	9.5	2.5	0	-5%	8	1
MIM	13/09/01	13:19	5	102	106	213	9.5	2.9	0	0	25-30	1
OCT	18/08/01	13:05	50	236	278	564	20	1.9	1	0	0-30	2
OTE	14/09/01	11:53	16	153	359	528	22	1.0	0	0	10-15	2
PED	13/09/01	13:55			2	2	3.5	5.0	1	0		0
SOL	17/09/01	12:32	7	187	147	341	10	2.0	1	0	10-20	1